RAPID MODELLING FOR FLEXIBLE CABLE BASED ON THE REVERSE ENGINEERING TECHNOLOGY

Hongwang Du[1], Wei Xiong[1], Haitao Wang[1] and Zuwen Wang[1]
[1] *Ship Electromechanical Equipment Institute, Dalian Maritime University, China*
E-mail: duhw_1984@dlmu.edu.cn

***ABSTRACT**: The assembly simulation of flexible cable based on physical modelling is a key link in virtual product design. However, due to the complicated large deformation of the flexible cable, there are two problems in the physical simulation model: one is that it is too difficult to carry out three-dimensional comparison validation between the simulation model and the real model, the other is that the render time of the simulation model is too long. Aiming at these two problems, a flexible cable geometry measurement and rapid modelling method based on non-contact 3D laser scanning technology is proposed. Targeting at the large deformation characteristics of flexible cable, this method establishes the activity testbed for two-end clamped cable, and point cloud data reflecting the cable geometry under different boundary conditions are gained with the help of a 3D laser scanner with coordinate measuring arms. Furthermore, the central axis of the cable is extracted on the basis of the point cloud data segmentation idea and the active contour model, and rapid geometry modelling and expression for flexible cable is realized based on the idea of sphere-moving surface. Finally, the cable geometry simulation system is developed based on an open source geometric kernel system, and the relevant models and algorithms are validated effectively.*
***KEYWORDS**: Flexible Cable, Geometry Measurement, Active Contour Model, Reverse Engineering, Sphere-moving Surface*

1 INTRODUCTION

With the development of complex products such as vehicles, ships and satellites, the proportion of cables becomes larger and larger. Cable becomes the key factor to determine the quality of products. Due to the variety and different shapes of cables, and limited assembly space in complex products, such problems as wrong installation, leakage, unreasonable layout or interference often occur in the assembly process (Liu, 2011), (Kuric,2015). The traditional design of cable is a two-dimensional serial mode, which is assembled by die or template method. The former can guarantee the accuracy, but the efficiency is low and the cost is high. The latter cannot guarantee the design parameters and layout accuracy of the cable (Grégoire, 2007; Wu, 2016).

With the development of CAD technology, current commercial CAD software (such as Solidworks, CATIA, Pro/E, etc.) all provides wiring module. The wiring principle of CAD is to use spline curve to fit the geometric shape of the cable, based on the key connection points confirmed in the electrical connection diagram. This method could provide the length of the cable, but the accuracy cannot be guaranteed and the assembly process cannot be verified (Wang, 2008; Xia, 2013). The emergence of virtual assembly technology provides a new idea for the digital design and assembly of cables. The framework of the virtual system for cables is shown in Figure 1 (Du, 2014).

It can be learned from the above figure that the most important technology involved in the virtual assembly system of the cable is mechanical modeling and numerical calculation. Judging from the current domestic and foreign literature, cables might be virtually assembled using the energy curve method, mass-spring method, rigid-body chain method, or the nonlinear mechanics of elastic rod method.

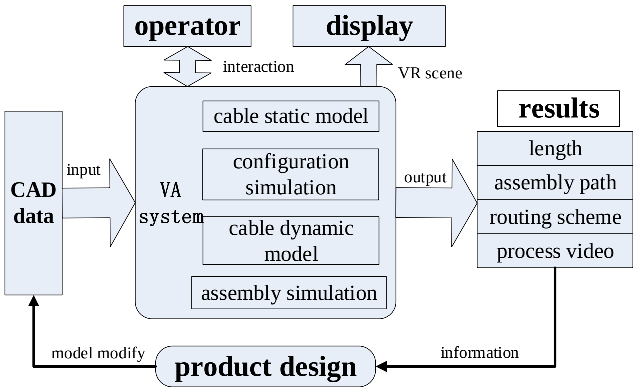

Figure 1. Cable VA system framework

For the energy curve method, the cable is viewed as the spline curve with potential energy. The cable meets the principle of energy minimization in a balanced state (Celniker, 1991). The principle of mass-spring method is to separate the cable into a series of massless points; two adjacent mass points are combined using an bending spring; and two neighboring bending springs are connected using rotation spring. The equilibrium form of the cable is figured out based on Newtonian mechanics principle (lv, 2017), (Loock, 2001). The rigid chain method considers the cable as a "globule-connecting rod" system and the equilibrium position of the cable is figured out based on the principle of flexible multi-body dynamics (Servin, 2008; Bretl, 2013). The method of elastic rod nonlinear mechanics was applied to analyze the DNA spiral shape in molecular biology at the earliest. Later, it was applied in the physical modeling of the cable. Its idea is that the geometry of the cable can be seen as the movement and rotation of the cross section along the center line. Based on the idea of dynamic analogy, the geometry problem of cable is transformed into the problem of spatial relative rotation between rigid body coordinate system (Hermansson, 2016; Liu, 2016).

It can be seen that there are many mechanical models for cable physical modeling. However, there are two common problems that have not been considered in the above studies. The first is the accuracy of the model is not verified from the experimental point of view, which cannot solve the problem of the oversizing of the cable length. The other is how to implement fast geometric modeling of cables in virtual assembly systems is not clarified, which is very important to the real-time performance of cable assembly simulation. Aiming at these two problems, this paper carries out study centering on the form measurement and rapid modeling of flexible cable.

In terms of the test, Jianhua Liu with Beijing Institute of Technology proposed a binocular vision motion detection method based on the centerline matching method to get the geometric characteristics of the cable (Liu, 2012). According to the pixels of the photos shot by two binocular cameras, the shape of the centerline was fitted as the geometric shape of the cable to be measured. Hermansson T used the laser scanner produced by Faro to get the 3D data of the cable, and compared the data of the cable with the simulation data to identify the material parameters of the cable (Hermansson, 2016). Additionally, geometric modeling of cable included the double geometric model and the spherical node-cylinder model; in the former model, the cable was represented by discrete fixed points and polygons with high accuracy, but the rendering efficiency was very low; while the latter had good real-time performance, and was suitable for cable assembly simulation, but the accuracy was poor.

Under the background of cable digital design and assembly, a flexible cable shape measurement and fast modeling method was put forward based on non-contact 3D laser scanning technology in this paper. This method can solve the two above two problems: one is the poor accuracy of cable length design and the other is the low efficiency of cable geometric form expression in simulation environment. The cable geometric shape measurement platform is established, and the point cloud data of the actual form of cables are obtained by using the non-contact laser scanner with coordinate measuring arm. The idea of point cloud data segmentation and active contour model are proposed to do the extraction of cable central axis. Fast geometric modeling and expression of flexible cable are carried out based on the idea of spherical moving surface. Finally, the model and algorithm are validated effectively in a cable shape simulation system developed by an open source geometric kernel system.

2 3D SCANNING MEASURING SYSTEM

Because of the flexibility of the cable, its spatial geometric shape is easy to change, which means that the cable shape cannot be determined by just several geometric parameters like the rigid body, which brings great difficulty to cable geometry measurement. The appearance of the non-contact laser scanner with coordinate measurement arm brings a feasible technology for the geometric measurement of the cable. The point cloud data of the cable are measured by the scanner, and the actual geometric shape of the cable can be quickly obtained by processing the point cloud data.

2.1 System structure

The flexible cable morphology test bench is shown in Figure 2.

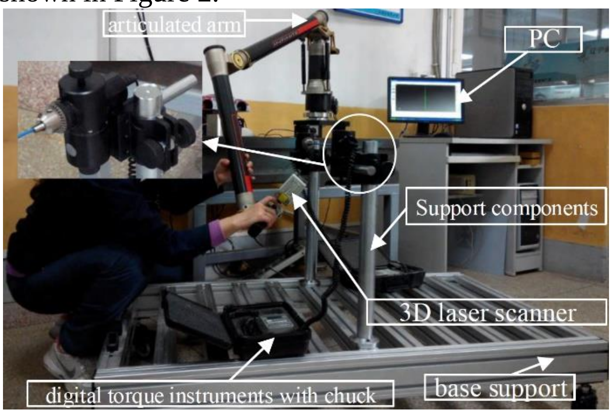

Figure 2. Clamped cable deformation test platform

The test bed consists of a base, two straight rods, two combined platforms, two chucks, two torque instruments, a coordinate arm laser scanner and a PC machine. The base is made of aluminum alloy profiles and can move horizontally in two directions to ensure that cables of different lengths can be measured. The combination of straight rods and combined platform can guarantee the movement of six degrees of freedom on both ends of the cable, and the straight rod and the combined platform have scales, so as to realize the rapid and accurate positioning of the relative position of the cable at both ends. The MGT-100Z digital torque instrument produced by Mark-10 Corporation in the USA has a measurement range of 14 N•cm and a precision of 0.01 N•cm. Each torque instrument has a chuck that easily clamps the cable with different diameter and the instrument can present the moment of force imposed by the chuck on the cable. The Romer-RA75-20SI 3D laser scanner with coordinate measurement arm produced by Corporation, USA has a measurement range of 2 m and a space length accuracy of 0.023 mm. PC is equipped with sweep test software to obtain point cloud data.

It can be seen that as long as the torque meter value and the location of the cable ends are given, the cable's geometry shape could be confirmed. Further, the laser scanner can get the geometric shape of the cable under different boundary conditions.

2.2 Measurement Experiment

In order to verify the feasibility of the test bench, this paper studies the cable shape change process with one end fixed and one end free moving. At the initial stage, the cable presents a straight line state, then one end is fixed, the other end moves toward the fixed end and the constraint torque is added, and the cable gradually appears bending and torsion. Material parameters of the cable are shown in Table 1.

Table 1. Material parameters for cable

Parameters	Value
Young modulus, N/m^2	3.89×10^9
Poisson ratio	0.25
Diameter, cm	0.2
Length, cm	30

The test procedure of cable shape is as follows:

1) Adjust the two combined platforms, move the cable to the fixed position and record the scale, and confirm the initial position vector of the cable;

2) Rotate the chuck, provide certain torque to the cable, and read the rotation angle value and the torque meter value;

3) After the two ends of the cable are completely fixed, the scanner scans the shape of the cable to obtain the point cloud data.

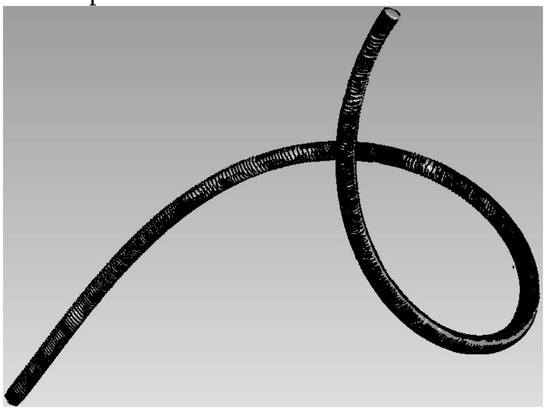

Figure 3. Point cloud data of cable geometry

The point cloud data obtained by laser scanner (taking a certain shape during the process as an example) is shown in Figure 3. It can be seen from the figure that the cable shape reflected by the point cloud data is completely consistent with the actual shape. In addition, the laser scanner has high scanning efficiency. The whole point cloud data of this example can be completed in less than two minutes (the number of points is 76,503).

3 CABLE CENTERLINE FITTING

In order to realize the fast reconstruction of the cable geometric shape, the idea of this paper is to divide the point cloud data into blocks. Each block is based on the active contour model to determine the point on the central axis. Finally, the cable centerline is obtained by fitting a series of discrete points using B-spline curve.

3.1 Point cloud data blocking

The point cloud data is very large, reaching tens of thousands or even hundreds of thousands. Direct data processing will lead to low efficiency for computer processing. Firstly, the point cloud data are partitioned into blocks, and then the redundant data and noise removal operations are initially carried out for each point cloud data block. In view of the point cloud data, the point cloud direction with larger span is chosen as the block direction. For the point cloud data in Figure 3, the X axis is taken as the direction of the point cloud data block. The point lineation represents a series of segmentation planes parallel to the X axis. The point cloud data is divided into several blocks, and the active contour model can be used to obtain an optimal centerline for each point cloud data.

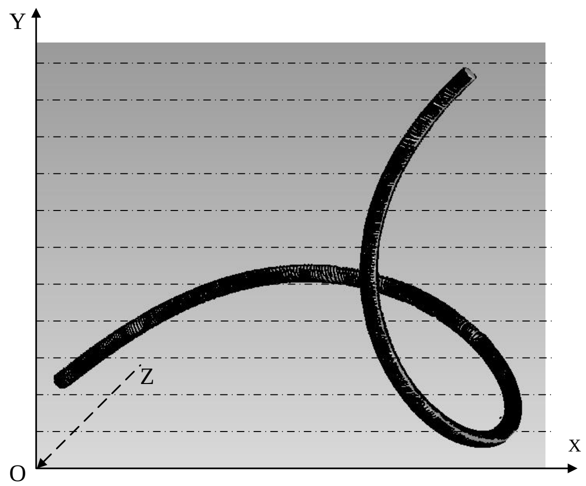

Figure 4. Block diagram of point cloud data

3.2 Cable centerline extraction

This section describes how to fit the centerline according to block point cloud data. $P=\{p_i\}\in R^3$ represents the block point cloud data (i=1,…, N), and φ stands for the fitted centerline.

After the point cloud data is partitioned, although the point cloud data for a single processing is reduced, it is still a problem to generate accurate centerline rapidly. The active contour model can effectively deal with the problem of 3D model reconstruction, and its advantage is that the feature extraction and feature description are combined into one. It is a novel top-down image target extraction method, and the extraction speed and accuracy of the cable centerline can be guaranteed simultaneously (Jacob, 2004; Zheng, 2015).

The active contour model considers that the cable centerline is a closed curve with minimum energy, and the model can minimize the following energy functional in the image space region.

$$E=\int_0^1\left(E_{\mathrm{int}}(\varphi)+E_{ext}(\varphi)\right)\mathrm{d}s \tag{1}$$

Where,

E means the total energy of the contour model;

E_{int} is the internal energy of the contour model;

E_{ext} refers to the external energy of the contour model;

s is the arc coordinate.

In order to obtain the accurate centerline shape, the active contour model requires an initial value, so it is necessary to estimate a rough model based on the point cloud data. A point sequence K is selected from the point cloud data of the cable surface, as the guide point to describe the shape of the cable. The rough model can be obtained by interpolating the K sequence, and then an initial solution is provided for the active contour model. In this paper, inner and outer energy of the active contour model are calculated respectively by the following formula.

$$E_{int}(\varphi)=\frac{1}{Nr^2}\sum_{i=1}^{N}\left\|\mathrm{d}(\varphi,p_i)-r_i\right\|^2+E_1(\varphi) \tag{2}$$

$$E_{ext}(\varphi)=\frac{1}{K-2}\sum_{k=2}^{K-1}\frac{v_{k-1}^T v_k}{\|v_{k-1}\|\|v_k\|}+E_2(\varphi) \tag{3}$$

Where, r is the nominal radius of a given cable, r_i is the radius of the corresponding point cloud data in the rough model, $d(\varphi, pi)$ is the closest distance from point cloud data p to curve φ, and v_k is the tangent of curve φ. E_1 and E_2 are penalty items, to make sure the fitted centerline is inside the point cloud.

The energy minimization problem is solved by using the steepest descent method in Mathematica. Figure 5 is the cable centerline based on the active contour model.

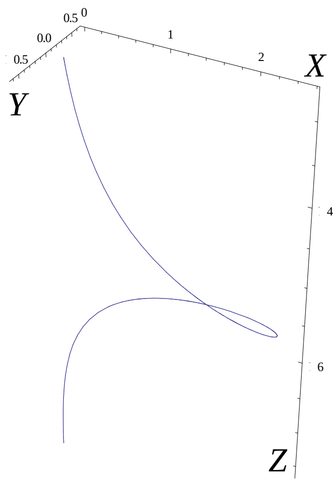

Figure 5. Fitted centerline

4 CABLE CENTERLINE FITTING

In the cable assembly simulation, the rapid solution and visual expression of the cable surface are realized according to the centerline shape to ensure the real-time performance of the cable assembly simulation. Surface modeling has always been a difficult problem in the field of computer graphics. Due to the characteristics of the large deformation of the cable flexibility, it becomes more and more difficult to realize the quick solving of the cable surface.

4.1 Principle of parameterization of cable surface

Aiming at the above problems, this paper presents a parametric modeling method for the cable surface with high efficiency and high robustness (Kim, 2003; Dayal, 2016). The definition of the cable surface is as follows: the cable surface is formed when the radius sphere variation function r(t) sweeps along the centerline curve function C(t), which is shown in Figure 6.

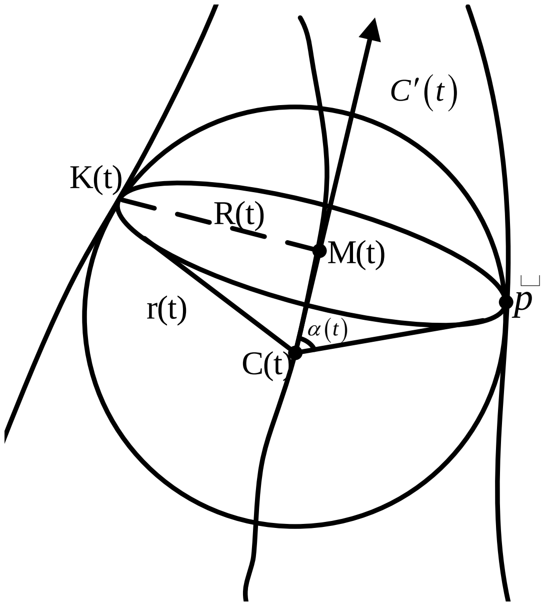

Figure 6. Sphere-moving surface schematic diagram

It can be seen from the diagram that any point ($\vec{p}$ =(x, y, z)) on the cable surface is located on the swept spherical surface with the radius of $r(t)$. And they satisfy the following equation:

$$\|\vec{p}-C(t)\|^2 - r(t)^2 = 0 \quad (4)$$

The point $\vec{p}$ is always on the envelope surface where the moving sphere is in. Therefore, it shall also satisfy the following equation:

$$[\vec{p}-C(t)]\cdot C'(t) + r(t)r'(t) = 0 \quad (5)$$

Formula (4) and Formula (5) define the relationship between the point, axis and the radius of the enveloping sphere on the cable surface section. The relationship of the three can define the cable surface.

Assume that $\alpha(t)$ is the included angle between the tangent vector and residual vector of the center line ($\vec{p}-C(t)$). The size of $\alpha(t)$ can be obtained based on Formula (6). The calculation of its cosine is as follows:

$$\cos\alpha(t) = \frac{[\vec{p}-C(t)]\cdot C'(t)}{\|\vec{p}-C(t)\|\|C'(t)\|} = -\frac{r'(t)}{\|C'(t)\|} \quad (6)$$

It is assumed that $S(t)$ is a moving sphere with a radius of $r(t)$ and a centerline of $C(t)$. When the sphere intersects with the cable surface, the intersecting lines form a closed circle K(t). The plane where the intersecting circle is located can be defined by the tangent vector $C'(t)$ of $C(t)$, which is obtained based on the space geometry knowledge. The central point $M(t)$ and radius R(t) of this intersecting circle can be figured out according to Formula (7) and Formula (8), which are shown as follows:

$$M(t) = C(t) + r(t)\cos\alpha(t)\frac{C'(t)}{\|C'(t)\|} = C(t) - r(t)r'(t)\frac{C'(t)}{\|C'(t)\|^2} \quad (7)$$

$$R(t) = r(t)\sin\alpha(t) = r(t)\frac{\sqrt{\|C'(t)\|^2 - r'(t)^2}}{\|C'(t)\|}$$

(8)

To sum up, taking $M(t)$ as the origin of coordinates, the cable surface can be expressed by the following parameterization formula.

$$K(t,\theta) = M(t) + R(t)\left[\cos\theta\vec{b}_1(t) + \sin\theta\vec{b}_2(t)\right] \quad (9)$$

Where, 0≤θ<2π. $\vec{b}_1(t)$ and $\vec{b}_2(t)$ are the other two base vectors of the section of the intersecting circle. Their calculation formulas are as follows:

$$b_1(t) = \frac{C'(t)\times C''(t)}{\|C'(t)\times C''(t)\|} \quad (10)$$

$$b_2(t) = \frac{C'(t)\times b_1(t)}{\|C'(t)\times b_1(t)\|} \quad (11)$$

4.2 Calculation of cable surface parameterization

It is assumed that the centerline of the cable surface is $C(t)$ and that the radius of the movable sphere is $r(t)$. In addition, $t_{min} \le t \le t_{max}$. It is also assumed that the cable surface is a regular surface. It can be concluded that $r(t)$ is larger than 0 and that $\|C'(t)\|^2 > r'(t)^2$. $C(t)$ is the second order continuous function.

Let the origin of the world coordinate system be $\vec{O}(O_x, O_y, O_z)$ and the $\vec{N}(t,\theta)$ be the normal vector of the cable surface $K(t,\theta)$. Then the three satisfy the following equation:

$$\vec{N}(t,\theta)\cdot\left[K(t,\theta) - \vec{O}\right] = 0 \quad (12)$$

According to mathematical knowledge, the normal vector of a surface can be calculated by the following relational equation:

$$\vec{N}(t,\theta) = \frac{\partial K(t,\theta)}{\partial t}\times\frac{\partial K(t,\theta)}{\partial\theta} \quad (13)$$

For the cable surface, the normal vector can be calculated from the following equation according to the spatial geometry relationship shown in Figure 6.

$$\vec{N}(t,\theta) = K(t,\theta) - C(t) \quad (14)$$

The following equation can be inferred from formula (12) and (14).

$$[K(t,\theta) - C(t)]\cdot\left[K(t,\theta) - \vec{O}\right] = 0 \quad (15)$$

Substitute formula (9) to the above formula and the following equation can be obtained:

$$A(t)\cos\theta + B(t)\sin\theta + D(t) = 0 \tag{16}$$

Where

$$A(t) = \vec{b}_1(t)\cdot\left[C(t) - \vec{O}\right]$$

$$B(t) = \vec{b}_2(t)\cdot\left[C(t) - \vec{O}\right]$$

$$D(t) = \frac{-r'(t)\left[C(t)-\vec{O}\right]\cdot C'(t) + r(t)\left\|C'(t)\right\|^2}{\left\|C'(t)\right\|\sqrt{\left\|C'(t)\right\|^2 - r'(t)^2}}$$

Based on formula (16), the following formula of θ can be derived.

$$\cos\theta = \frac{-A(t)D(t) \pm B(t)\sqrt{A(t)^2 + B(t)^2 - D(t)^2}}{A(t)^2 + B(t)^2}$$

$$\sin\theta = \frac{-A(t)\cos\theta - D(t)}{B(t)} \tag{17}$$

In conclusion, any point $\vec{p}$ on the cable surface can be figured out based on the following equation.

$$\vec{p} = M(t) + R(t)\left[c(t)\vec{b}_1(t) + s(t)\vec{b}_2(t)\right] \tag{18}$$

Where,

$$c(t) = \frac{-A(t)D(t) \pm B(t)\sqrt{A(t)^2 + B(t)^2 - D(t)^2}}{A(t)^2 + B(t)^2}$$

$$s(t) = \frac{-A(t)c(t) - D(t)}{B(t)}$$

5 REALIZATION OF CABLE RAPID MODELING SYSTEM

The above respectively introduces the cable shape rapid scanning, the centerline extraction and the drawing of cable surface. No matter from the perspective of cable design or from the angle of testing contrast analysis, the cable geometry model is required to be a standard CAD format, which is the premise condition. Therefore, a cable geometric shape fast generating module is developed in this paper based on Open Cascade (DING, 2014) on the virtual assembly system platform and under the development environment of Visual Studio 2015, so as to verify the effectiveness of the model and algorithm proposed above.

5.1 System development process

The system development process is shown in Figure 7.

Initialize the point cloud data; point cloud data blocking; extract the centerline coarse model; active contour model-energy calculation; energy optimization-extracting the centerline-generating BSpline curve; format conversion; define the sweep volume variable aPipe; display the curve; perform scanning; acquire the scanning surface; format conversion; display the surface.

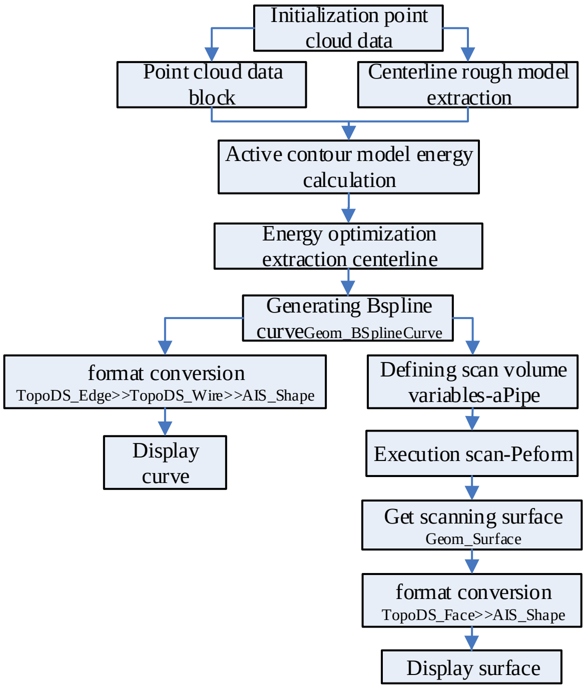

Figure 7. Development flow chart of cable rapid modeling system

The explanation of the development process of the cable fast modeling system is as follows: Firstly, according to the point cloud data obtained by the scanner, on the one hand, a rough model of the centerline is generated by virtue of the reverse engineering software, and on the other hand, the point cloud data is blocked along the maximum contour direction; secondly, for each block of point cloud data, the centerline of each segment is fitted based on the active contour model, and the midpoint of each Central Line is viewed as the key point of this cable. Then, the curve fitting function provided by OCC is used to generate the centerline in the b-spline form based on the above key points; finally, the user-defined sphere moving sweep function is applied to realize the geometrical expression of the cable surface. OCC can realize the output in standard CAD format (*.step).

5.2 Algorithm implementation

The pseudo code of the rapid modeling algorithm of the cable surface is shown below.

input (x_i, y_i, z_i), for i=1,…,n
/*input point cloud data*/
max $(x_n-x_1,\ y_n-y_1,\ z_n-z_1)$
b[j], for j=1,…,m /*point cloud data blocking */

$$E_{int}(\varphi) = \frac{1}{mr^2}\sum_{i=1}^{m}\left\|\mathrm{d}(\varphi, p_i) - r_i\right\|^2 + E_1(\varphi)$$

$$E_{ext}(\varphi)=\frac{1}{K-2}\sum_{k=2}^{K-1}\frac{v_{k-1}^{T}v_k}{\|v_{k-1}\|\|v_k\|}+E_2(\varphi)$$

$$E_{sum}=E_{\text{int}}(\varphi)+E_{ext}(\varphi)$$

/*calculate the internal energy and external energy of each block of point cloud and sum up*/

min E_{sum}

$$\nabla E_{sum}(\varphi)=\left[\frac{\partial E_{sum}}{\partial\varphi_1}\quad\frac{\partial E_{sum}}{\partial\varphi_2}\quad\cdots\quad\frac{\partial E_{sum}}{\partial\varphi_n}\right]^T$$

/*gradient*/

input ${E_{sum}}^1$

/*initial value*/

${E_{sum}}^{i+1}={E_{sum}}^{i}+\lambda\cdot\nabla E_{sum}$

/*search direction definition*/

if ${E_{sum}}^{i+1}-{E_{sum}}^{i}<\varepsilon$

/*determination*/

Geom_BSplineCurve

End /*spline interpolation generating center line*/

/*extract the cable centerline using active contour method*/

Input:

C(t)=(x(t),y(t),z(t)), /*input centerline*/

r(t)=r, /*The cable radius is a constant*/

$\vec{O}=(O_x,O_y,O_z)$,/*define the original point of the world coordinate system */

begin

for each $t_*\in\{t\,|A(t)=0\ and\ B(t)=0\}$ do

if $D(t_*)=0$ then

draw a circle $K(t_*,\theta),0\le\theta<2\pi$;

$$T=\{t_{\min},t_{\max}\}\cup\{t|$$
$$((\vec{O}-C(t))\cdot C'(t)^2+2r(t)r'(t)(\vec{O}-C(t))\cdot C'(t)$$
$$-\|\vec{O}-C(t)\|^2(C'(t)^2-r'(t)^2)+\|C'(t)\|^2r(t)^2=0;$$

sort *t* values in *T*: *T*= $T=\{t_i\,|0\le i<n\}$;

for *i*=1 to *n*-1 do begin

$t_*=(t_{i-1}+t_i)/2$;

if $A(t_*)^2+B(t_*)^2-D(t_*)^2\ge 0$ then begin

for $t_{i-1}\le t\le t_i$, draw a curve

$M(t)+R(t)\left[c_a\vec{b}_1(t)+s_a\vec{b}_2(t)\right]$, where

$$c_a=\frac{-A(t)D(t)+B(t)\sqrt{A(t)^2+B(t)^2-D(t)^2}}{A(t)^2+B(t)^2}$$

and $s_a=\dfrac{-A(t)c_a-D(t)}{B(t)}$;

for $t_{i-1}\le t\le t_i$, draw a curve

$M(t)+R(t)\left[c_b\vec{b}_1(t)+s_b\vec{b}_2(t)\right]$, where

$$c_b=\frac{-A(t)D(t)-B(t)\sqrt{A(t)^2+B(t)^2-D(t)^2}}{A(t)^2+B(t)^2}$$

and $s_b=\dfrac{-A(t)c_b-D(t)}{B(t)}$;

end

end

end

/*sphere moving surface sweeping*/

TopoDS_Edge /*centerline identification*/

TopoDS_Wire /*Topology expression of the centerline*/

AIS_Shape /*centerline display*/

Geom_Surface /*cable surface identification*/

TopoDS_Face /*Topology expression of the cable surface*/

AIS_Shape /*cable surface display*/

5.3 Case Analysis

In order to verify the effectiveness of the model and algorithm proposed in this paper, the calculating example mentioned in section 1.2 was taken as the research object. When one end of the cable is constantly moving towards the fixed end and the torque is gradually increasing, two middle postures are taken as the example. The point cloud data of these two postures are obtained through scanning. After point cloud data blocking, centerline extraction and cable surface expression, two geometric shapes of the cable surface are obtained, which are shown in Figure 8.

For the sake of visual display, the scanned sphere is shown in the key point of the centerline. The cable surface model established can be exported in the form of *.Step, which can be easily read out by any 3D-CAD software. Therefore, the 3D contrast verification between the simulation model and actual model can be implemented. It can be seen from the figure that the complete modeling of flexible cable can be realized based on converse engineering technology. In addition, it takes an average of 9ms to generate the cable surface based on the sphere motion scanning idea. This modeling idea can also be used in the assembly simulation of cables. And it can satisfy the requirement of real time performance of the cable assembly simulation.

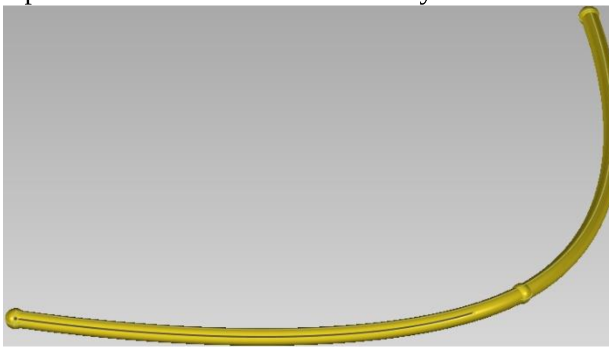

a) Middle Postures

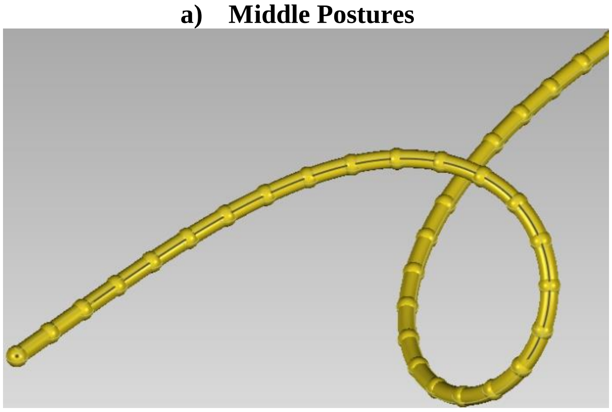

b) final form

Figure 8. Geometric shape of the measured cable surface

6 CONCLUDING REMARKS

(1) In view of the flexible cable geometry measurement difficulties and the low efficiency of curved surface modeling, a flexible cable geometry measurement and rapid modelling method based on non-contact 3D laser scanning technology is proposed. The complete measurement and three-dimensional topological expression of the cable geometry are realized, and the cable surface modeling system is developed to verify the effectiveness of the method.

(2) In view of the blocked point cloud data, the energy model of each block of point cloud data is built based on the active contour model. The position of each centerline is confirmed using the steepest descent method. Taking the midpoint of each centerline as the key point, the cable centerline is finally extracted out based on the spline curve interpolating idea.

(3) The cable surface is obtained by the sweeping of the sphere along the centerline. The established cable surface model can be exported in the standard CAD format *.step. Therefore, the 3D contrast verification between the simulation model and actual model can be implemented. It takes an average of 9ms to finish the cable surface modeling. This modeling idea can also be used in cable assembly simulation. And it can satisfy the requirement of real time performance of the cable assembly simulation. The research results in this paper is of strong guiding significance and reference value for cable geometry measurement and cable assembly simulation

7 ACKNOWLEDGEMENTS

The work in this paper was supported by the National Natural Science Foundation of China (51175053) and the Fundamental Research Funds for the Central Universities of China (3132016353 and 3132016073) and Liaoning Provincial Natural Science Foundation of China (201601068).

8 REFERENCES

► Bretl T., McCarthy Z. (2013). Mechanics and quasi-static manipulation of planar elastic kinematic chains. IEEE Transactions on Robotics, 29(1): 1-14.

► Celniker G., Gossard D. (1991). Deformable curve and surface finite-elements for free-form shape design. ACM SIGGRAPH computer graphics, 25(4): 257-266.

► Dayal P.A.S., Raju G.S.N., Mishra S. (2016). Pattern synthesis using accelerated particle swarm optimization, Modelling, Measurement and Control A, 89(1), 58-76.

► Ding H., Wang Z. (2014). Development and Research of CAD System Based on an Open CASCADE Platform. Journal of Southwest University of Science and Technology, 29(2): 72-76.

► Du H.W. (2014). Physical Modeling and Configuration Simulation for Flexible Cable. Dalian Maritime University.

► Grégoire M, Schömer E. (2007). Interactive simulation of one-dimensional flexible parts. Computer-Aided Design, 39(8): 694-707.

► Hermansson T., Bohlin R., Carlson J.S. (2016). Automatic routing of flexible 1D components with functional and manufacturing constraints. Computer-Aided Design, 79(1): 27-35.

► Hermansson T., Vajedi S., Forsberg T. (2016). Identification of Material Parameters of Complex Cables from Scanned 3D Shapes. Procedia Cirp, 43(1): 280-285.

► Jacob M., Blu T., Unser M. (2004). Efficient energies and algorithms for parametric snakes. IEEE transactions on image processing, 13(9): 1231-1244.

► Kim K.J., Lee I.K. (2003). Computing isophotos of surface of revolution and canal surface. Computer-Aided Design, 35(3): 215-223.

► Kuric I., Císar M., Novosád M., Krchova D., Grozav S. (2015). Experimental device for practicing routines of machine tool precision

measurement, Academic Journal of Manufacturing Engineering, 13(1), 39-44.
► Lii J.S., Liu J.H., Jin W.T. (2016). A Virtual Layout Design Method of Motional Cable in Stabilized Platform. Journal of Mechanical Engineering, 52(21): 111-119.
► Liu J.H., Wang X.Y., Zhang T. (2012). Motion Detection Method of Flexible Cable Harness Based on Binocular Vision and its Error Analysis. Transactions of Beijing Institute of Technology, 32(8): 795-800.
► Liu J.H., Zhao T., Wang C.S. (2011). Motional Cable Harness Physical Characteristic Oriented Modeling and Kinetic Simulation Technology in Virtual Environment. Journal of Mechanical Engineering, 47(9): 117-124.
► Loock A., Schömer E., Stadtwald I. (2001). A virtual environment for interactive assembly simulation: From rigid bodies to deformable cables. //5th World Multiconference on Systemics, Cybernetics and Informatics (SCI'01). 3: 325-332.
► Lv N., Liu J., Ding X. (2017). Physically based real-time interactive assembly simulation of cable harness. Journal of Manufacturing Systems, 43(1): 385-399.
► Mm H.Q., Zhang J.R., Zhang X.Y. (2013). Cable Deformation Simulation Based on B-Spline Curve. Computer Engineering and Science, 34(11): 91-95.
► Servin M., Lacoursiere C. (2008). Rigid body cable for virtual environments. IEEE transactions on visualization and computer graphics, 2008, 14(4): 783-796.
► Wang J.F., Yan J., Wu K. (2008). Key Technologies on the Cable Harness Assembly Planning System Based on Pro/E. Chinese Mechanical Engineering, 19(13): 1565-1569.
► Wu D.Q., Tang L.X., Lia H.Y., Ouyang L.J. (2016). A co-evolutionary particle swarm optimization with dynamic topology for solving multi-objective optimization problems, Advances in Modelling and Analysis A, 53(1), 145-159.
► Xia P., Lopes A.M., Restivo M.T. (2013). A review of virtual reality and haptics for product assembly: from rigid parts to soft cables. Assembly Automation, 33(2): 157-164.
► Zheng G.L., Zhang L., Zhuan X.T., Shang X.D. (2015). A measuring method for three-dimensional turbulent velocities based on vector decomposition and synthesis, International Journal of Heat and Technology, 33(4), 51-60.